PCCP

Cite this: *Phys. Chem. Chem. Phys.*, 2012, **14**, 9696–9701

www.rsc.org/pccp

PAPER

Photo-impulsive reactions in the electronic ground state without electronic excitation: non-photo, non-thermal chemical reactions†

Izumi Iwakura,*[ab] Atsushi Yabushita,[c] Jun Liu,[d] Kotaro Okamura[d] and Takayoshi Kobayashi[cd]

Received 27th February 2012, Accepted 18th May 2012
DOI: 10.1039/c2cp40607a

Allyl phenyl ether has an absorption band in the ultraviolet region (λ < 400 nm); therefore, irradiation with few-optical-cycle ultraviolet pulses (λ = 360–440 nm) causes a transition to the ultraviolet band, which leads to an electronic state and a photo-Claisen rearrangement (radical reaction) in the electronic excited state. However, the reaction scheme of allyl phenyl ether under irradiation with few-optical-cycle visible pulses (λ = 525–725 nm) was determined to be same as that of the thermal Claisen rearrangement ([3,3]-sigmatropic rearrangement), which is symmetry-allowed in the electronic ground state. Photo-excitation with few-optical cycle visible pulses below the absorption band induces a photo-impulsive reaction in the electronic ground state without electronic excitation, of which the trigger scheme is different from that of photoreaction or thermal-reaction. The photo-impulsive reaction in the electronic ground state is highly possible as a novel reaction scheme.

1. Introduction

Chemical reactions can be generally classified into two groups; photoreactions and thermal reactions. When a chemical compound absorbs light of which the photon energy is equal to the electronic transition energy, the compound is excited into an electronic excited (EE) state. The excitation of the electronic state increases lability, which triggers a photoreaction in the EE state. In contrast, thermal reactions proceed in the electronic ground (EG) state due to thermal excitation of molecular vibrational modes of the EG state. Therefore, the frontier orbital that participates in thermal reactions differs from that for photoreactions, which frequently causes differences in reactivity.

For example, irradiation of allyl phenyl ether (APE) with ultraviolet (UV) light at its absorption band (λ < 400 nm) causes a photo-Claisen rearrangement *via* a radical intermediate and produces not only *o*-allyl phenol, but also *p*-allyl phenol and phenol (Scheme 1(1)).[1] In contrast, thermal excitation of APE proceeds with a [3,3]-sigmatropic rearrangement, in which a six-membered transition state appears under a supra–supra facial reaction and produces 6-allyl-cyclohexa-2,4-dienone. The 6-allyl-cyclohexa-2,4-dienone converts itself into the more stable *o*-allyl phenol product under keto–enol tautomerism (Scheme 1(2)).[2]

We have previously reported[3,4] that when the pump photon energy is lower than the minimum electronic transition energy, molecular vibrational modes of the EG state are excited *via* an induced Raman process, which triggers the reaction in the EG state without converting photon energy to thermal energy.[5–7] In the present work, we have applied selective triggers for the Claisen rearrangements of APE. As a result, the Claisen rearrangement in the EE state (photoreaction) and that in the EG state (photo-impulsive reaction in the EG state) can be selectively induced using few-optical-cycle pulses of UV and visible radiation, respectively (Fig. 1). It was confirmed that the photo-impulsive reaction pathway in the EG state (as for thermal reactions) is different from that in the EE state (as for photoreactions).

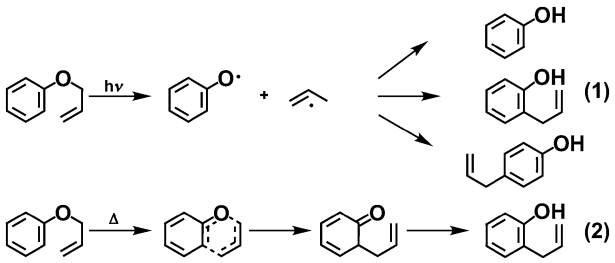

Scheme 1

[a] *Innovative use of light and materials/life, PRESTO, JST, 4-1-8 Honcho, Kawaguchi, Saitama 332-0012, Japan. E-mail: iwakura@ils.uec.ac.jp*
[b] *Department of Chemistry, Graduate School of Science, Hiroshima University, 1-3-1 Kagamiyama, Higashi-Hiroshima, Hiroshima 739-8526, Japan*
[c] *Department of Electrophysics, National Chiao-Tung University, Hsinchu 300, Taiwan*
[d] *University of Electro-Communications, 1-5-1 Chofugaoka, Chofu, Tokyo 182-8585, Japan*
† Electronic supplementary information (ESI) available. See DOI: 10.1039/c2cp40607a

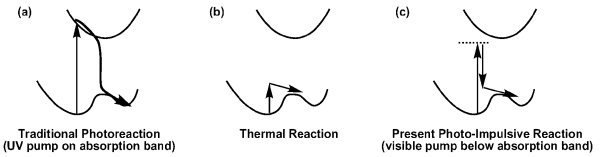

Fig. 1 The three reaction mechanisms under investigation: (a) traditional photoreaction in the electronic excited state; (b) thermal reaction in the electronic ground state; (c) the present photo-impulsive reaction in the electronic ground state.

2. Experimental

2.1. Few-optical-cycle ultraviolet pulses

A hollow-fiber compression system was used to obtain few-optical-cycle broadband UV pulses.[8] A Ti : sapphire regenerative amplifier (Coherent, Legend Elite-USP; 2.5 mJ, 35 fs, 1 kHz at 800 nm) was wavenumber-doubled in a beta barium borate (BBO) crystal to generate second-harmonic laser pulses at 400 nm, which were focused into a hollow fiber. The pulses were spectrally broadened in the fiber to 360–440 nm and the time duration was compressed to as short as 8 fs using a pulse compressor. The focal areas of the pump pulse and the probe pulse were 100 and 75 μm^2, respectively.

2.2. Few-optical-cycle visible pulses

A Ti : sapphire regenerative amplifier (Spectra Physics, Spitfire; 150 μJ, 100 fs, 5 kHz at 805 nm) was used to pump a non-collinear optical parametric amplifier (NOPA) to obtain few-optical-cycle broadband visible pulses.[9] The signal pulse was amplified by the double-pass NOPA in the broadband spectral region from 525 to 725 nm and the pulse compressor compressed the pulse duration to 5 fs. The focal areas of the pump pulse and the probe pulse were 100 and 75 μm^2, respectively.

2.3. Sample cell

A liquid cell with an optical path length of 1 mm was used to contain the sample during measurement at 295 ± 1 K. Neat liquid of APE (CAS: 1746-13-0, Tokyo Chemical Industry) was stored in the cell for use as a sample. Under irradiation by the UV pulses, light absorption by the sample causes thermal accumulation and bubbling if the pulses irradiate a fixed point. Therefore, during UV pulse irradiation, the sample cell was continuously translated in the plane perpendicular to the probe beam. The shape of the translation trajectory was near-circular and octagon-like, and the speed was *ca.* 5 mm s^{-1}, which corresponds to a sample displacement of *ca.* 10 μm during the pulse period of 1 ms. This procedure reduced the probability of sample photodamage to a minimum.

2.4. Pump–probe measurement

The probe pulse was dispersed using a polychromator (300 grooves per mm, 500 nm blazed for visible pulses and 300 nm blazed for UV pulses). The dispersed probe wavelength components were guided to 128 avalanche photodiodes *via* a 128-channel bundled fiber. The signal-to-noise ratio was improved by coupling the signals of the avalanche photodiodes to a 128-channel lock-in amplifier.

2.5. Quantum chemical calculation

The Gaussian 03 program[10] was used for the calculations without assuming symmetry. Geometric optimization was performed using the B3LYP/6-311 + G(d,p) method and basis set (5d functions were used for the d orbital). Wavenumber calculations were performed for all of the obtained structures at the same level. All the frequencies were confirmed as real for the ground states and one imaginary wavenumber for the transition state (TS). Vectors of the imaginary frequencies directed the reaction mode and intrinsic reaction coordinate calculations were further performed to confirm that the obtained TSs were on the saddle points of the energy surface between the reactant and product.

3. Results

3.1. Vibrational dynamics in the reaction under few-optical-cycle ultraviolet pulse irradiation (see Fig. 1a)

APE has absorption bands in the UV region ($\lambda < 400$ nm); therefore, irradiation with few-optical-cycle UV pulses (λ = 360–440 nm) caused photo-excitation at the absorption band, which excited the electronic state of APE and photo-Claisen rearrangement (radical reaction) proceeded in the EE state (Fig. 2).

A pump–probe measurement of APE was performed to investigate the photo-Claisen rearrangement using the few-optical-cycle UV pulses (see Section 2.1). Fig. 3a shows a two-dimensional view of the observed time-resolved transmission change ($\Delta T/T$), which indicates the appearance of an induced absorption at 1.8 ps after photo-excitation.

A fast Fourier transform (FFT) of $\Delta T/T$ between 200 and 1200 fs was calculated using the Hanning window function, as shown in Fig. 3b. The calculated FFT power spectrum has peaks at 814, 993, 1278, and 1644 cm^{-1}. Spectrogram analysis[11] was performed using a Blackmann window function with a 400 fs full width at half maximum (FWHM) to elucidate the dynamics of the vibrational modes (see Fig. 3c).

Vibrational modes at 1007, 1080, 1186, 1320, 1487, and 1670 cm^{-1} were evident immediately after the photo-excitation. The highest peak at 1007 cm^{-1} is separated into two components; one exhibited a red shift and the other did not shift until 2.5 ps after photo-excitation. At a delay time of 1.7 ps, the peak at 1670 cm^{-1} disappeared and a new peak appeared at 1533 cm^{-1}. The peak at 1080 cm^{-1} underwent a gradual blue-shift with generation of a new peak at 1425 cm^{-1}.

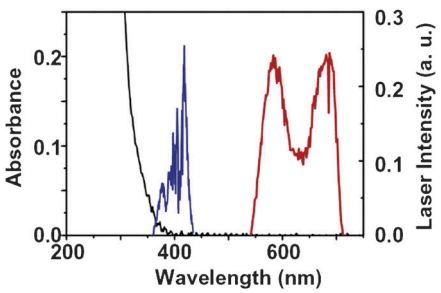

Fig. 2 An absorption spectrum of allyl phenyl ether (black curve), and laser spectra of the few-optical-cycle UV (blue curve) and visible (red curve) pulses.

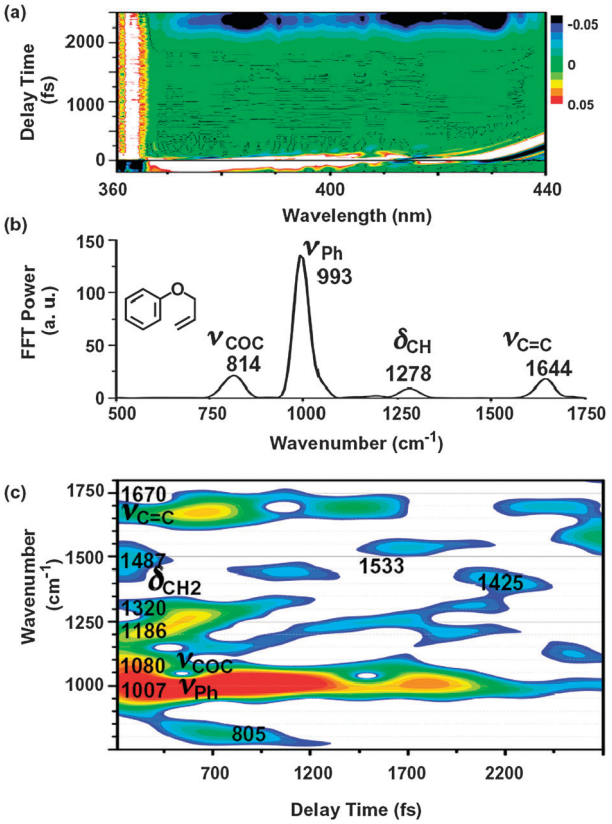

Fig. 3 Experimental results observed using UV pulses. (a) A two-dimensional display of the change in absorbance of allyl phenyl ether as a function of probe delay time and wavelength. (b) A FFT power spectrum of the oscillating components of the time-resolved absorbance change. (c) The observed time dependence of the vibrational spectra.

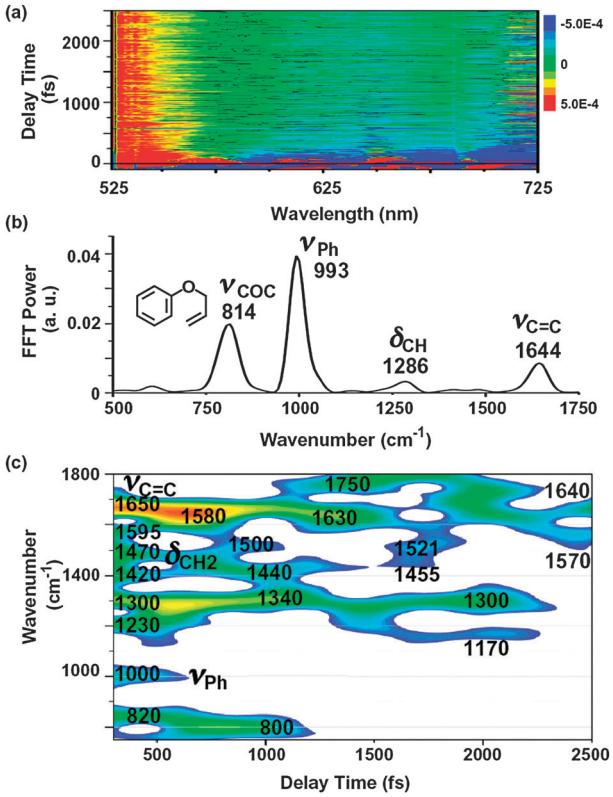

Fig. 4 Experimental results observed using visible pulses[4]. (a) A two-dimensional display of the change in absorbance of allyl phenyl ether as a function of the probe delay time and wavelength. (b) A FFT power spectrum of the oscillating components of the time-resolved absorbance change. (c) The observed time dependence of the vibrational spectra.

3.2. Vibrational dynamics in the reaction under few-optical-cycle visible pulse irradiation (see Fig. 1c)

The pump–probe measurement was also performed using few-optical-cycle visible pulses (see Section 2.2). The photon energy of the visible pulses (λ = 525–725 nm) is lower than the minimum electronic transition energy of APE (λ < 400 nm) (Fig. 2).

A two-dimensional view of the measured $\Delta T/T$ is shown in Fig. 4a. The standard deviation of the induced absorbance difference ΔA, oscillating around the estimated zero absorbance change, was less than 5×10^{-5}, which is negligible when compared with the oscillation amplitude ($\delta\Delta A$) of 3×10^{-4}. The deviation from zero is due to a very small accumulated steady-state population of EGs.

The FFT of $\Delta T/T$ between 200 and 1200 fs was calculated using a Hanning window function, as shown in Fig. 4b. The calculated FFT power spectrum has peaks at 814, 993, 1286, and 1644 cm^{-1}. Spectrogram analysis was performed using a Blackmann window function with 400 fs-FWHM to elucidate the dynamics of the vibrational modes (see Fig. 4c).

Vibrational modes at 820, 1000, 1230, 1300, 1420, 1470, 1595, and 1650 cm^{-1} were evident immediately after photo-excitation. The peak at 1000 cm^{-1} disappeared at a delay time of 700 fs without any shift in wavenumber. The mode of 1650 cm^{-1} underwent a gradual red shift with generation of a new peak at 1580 cm^{-1} at a delay time of 750 fs. A new peak appeared at 1750 cm^{-1} after a delay time of 1 ps and disappeared at a delay time of 2 ps.

3.3. Theoretical vibrational dynamics of the photo- and thermal reactions

A density functional formalism was used to calculate molecular vibrational changes in the photo-Claisen rearrangement and the thermal Claisen rearrangement. Fig. 5 shows a measured Raman spectrum of APE and the calculated wavenumbers of the molecular vibrational modes. The measured results show that symmetric stretching of the phenyl group, C–O–C symmetric stretching of the ether group, C–H deformation of the phenyl group, C–O–C stretching of the ether group and C–H_2 twisting of the methylene group, C–H deformation of the allyl group, C–H_2 wagging of the methylene group, C–H_2 scissoring of the allyl group, C═C stretching of the phenyl group, and C═C stretching of the allyl group appear at 997, 1032, 1173, 1244, 1291, 1419, 1458, 1595, and 1648 cm^{-1}, respectively. The values in Fig. 5 (the measured Raman wavenumbers and the corresponding calculated wavenumbers) were used to estimate scaling factors (see Table 1).

In the photo-Claisen rearrangement (see Table 2), an allyl radical appears with a C–C$^{\bullet}$ stretching mode at 1510 cm^{-1},

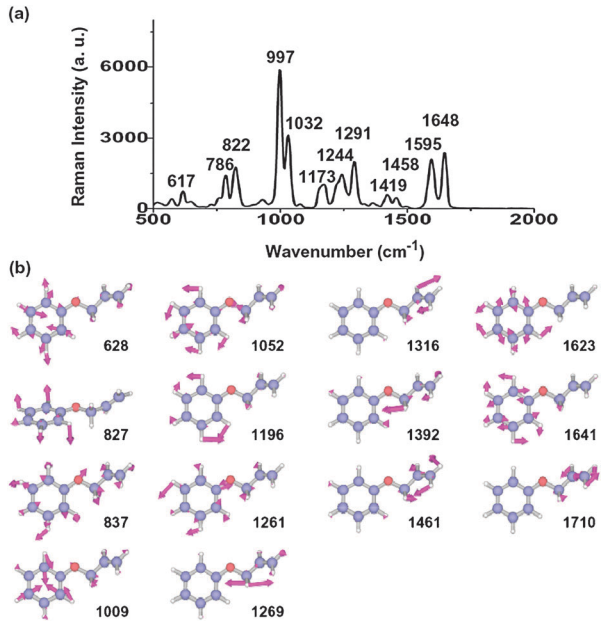

Fig. 5 (a) Measured Raman spectrum of allyl phenyl ether. (b) Molecular vibrational modes calculated using B3LYP/6-311+G(d,p).

and a phenoxy radical appears with ring stretching of the phenyl group (805 and 1008 cm^{-1}) and C–O$^{\bullet}$ stretching (1480 cm^{-1}).

In the thermal Claisen rearrangement (see Table 3), a six-membered structure appears with C–O–C asymmetric stretching of the ether group (815 cm^{-1}), C–H deformation of the allyl group (1319 cm^{-1}), and C=C stretching in the allyl and phenyl groups (1542 cm^{-1}). The subsequent intermediate, 6-allyl-cyclohexa-2,4-dienone, has a C–H_2 twisting of the methylene group, C–H deformation of the allyl group, C–H_2 scissoring deformation of the allyl group, C=C stretching of the allyl group, and C=O stretching at 1196, 1300, 1448, 1637, and 1720 cm^{-1}, respectively. The final product, *o*-allyl phenol, appears with C=C stretching of the phenyl group (1584 cm^{-1}) and C=C stretching of the allyl group (1635 cm^{-1}).

4. Discussion

4.1. Photochemically-allowed Claisen rearrangement of allyl phenyl ether by few-optical-cycle ultraviolet pulse irradiation

APE has an absorption band at wavelengths shorter than 400 nm. Therefore, irradiation with few-optical-cycle UV pulses having a broadband spectrum of 360–440 nm excites the electronic state of APE to the EE state. Molecular vibrations are coherently excited *via* vibronic interaction, which enables observation of the EE state dynamics *via* molecular vibrations.

Fig. 3c shows a calculated spectrogram that reflects the vibrational dynamics. The observed vibrational dynamics of the photoreaction during reaction under few-optical-cycle UV pulses were in agreement with the theoretical vibrational dynamics of the photoreaction, which confirms that the vibrational dynamics follow those for the photoreaction, as explained in the following.

The C=C stretching of the allyl group was observed at 1670 cm^{-1} immediately after the photo-excitation and then disappeared at a delay time of 1.7 ps when the allyl radical was produced, and a new peak of C–C$^{\bullet}$ stretching of the allyl radical appeared at 1533 cm^{-1}. The peak of symmetric stretching in the phenyl group observed at 1000 cm^{-1} just after photo-excitation was separated into two modes as the phenoxy radical was generated; one of the two modes was red-shifted to 805 cm^{-1} and the other experienced no change in wavenumber. The peak observed at 1080 cm^{-1} just after photo-excitation was gradually blue-shifted with generation of the C–O$^{\bullet}$ group and a new peak at 1425 cm^{-1} appeared at a delay time of *ca.* 2 ps.

The vibrational mode dynamics indicate that active radical species are generated at 1.8–2.0 ps after photo-excitation. Phenoxy radicals have an absorption band at 360–420 nm[12] and the transitional absorption appeared at a delay time of 1.8 ps (see Fig. 3a). Thus, irradiation with few-optical-cycle pulses induces photoreaction by excitation of the electronic state into the EE state if the laser spectrum overlaps with the absorption band of the sample that corresponds to its electronic transition.

4.2. Thermally-allowed Claisen rearrangement of allyl phenyl ether by few-optical-cycle visible pulse irradiation

The reaction induced by irradiation with few-optical-cycle visible pulses (525–725 nm) (Fig. 4c) was completely different from that for the few-optical-cycle UV pulse irradiation (Fig. 3c). The observed vibrational dynamics were in agreement with the theoretical vibrational dynamics of the thermal Claisen reaction (Table 3), which indicates that the reaction is the thermally-allowed Claisen rearrangement in the EG state, as explained in the following.

The symmetric stretching of the phenyl group observed at 1000 cm^{-1} immediately after the photo-excitation disappeared at a delay time of *ca.* 700 fs. The C–H_2 deformation of the methylene group observed at 1230 and 1420 cm^{-1} also disappeared at the same delay time of 700 fs. The C=C stretching

Table 1 Wavenumber scaling factors of the vibrational modes

	Molecular vibrational mode cm^{-1}													
	δ_{Ph} Ph	δ_{CH} Ph	δ_{Ph} Ph	δ_{Ph} Ph	ν_{COC} Ether	δ_{CH} Ph	ν_{COC} Ether	δ_{CH_2} Methylene	δ_{CH} Allyl	δ_{CH_2} Methylene	δ_{CH_2} Allyl	$\nu_{C=C}$ Ph	$\nu_{C=C}$ Ph	$\nu_{C=C}$ Allyl
Exp.	617	786	822	997	1032	1173	1244	1244	1291	1419	1458	1595	1595	1648
Calc.	628	827	837	1009	1052	1196	1261	1269	1316	1392	1461	1623	1641	1710
S.F.[a]	0.98	0.95	0.98	0.99	0.98	0.98	0.99	0.98	0.98	1.02	1.00	0.98	0.97	0.96

[a] Scaling Factor (S.F.) = Experimental wavenumber (Exp.)/Calculated wavenumber (Calc.).

Table 2 Calculated vibrational wavenumbers of chemical species involved in the photo-Claisen rearrangement of allyl phenyl ether

	Calculated molecular vibration wavenumber[a] cm^{-1}											
Compound	ν_{Ph} Ph		ν_{CCC} Allyl	ν_{COC} Ether	δ_{CH} Ph	δ_{CH_2} Methylene	δ_{CH} Allyl	δ_{CH_2} Methylene	δ_{CH_2} Allyl	ν_{CCC} Allyl	$\nu_{C=C}$ Ph	$\nu_{C=C}$ Allyl	$\nu_{C=O}$
Reactant		1009		1052	1196	1269	1316	1392	1461		1641	1710	
Allyl radical			1036					793		1269		1510	
Phenoxy radical	805	1008		1480	1166						1585		

[a] Not scaled by any scaling factor.

Table 3 Calculated vibrational wavenumbers of chemical species involved in the thermal Claisen rearrangement of allyl phenyl ether

	Calculated molecular vibration wavenumber[a] cm^{-1}									
Compound	δ_{Ph} Ph	ν_{Ph} Ph	ν_{COC} Ether	δ_{CH_2} Methylene	δ_{CH} Allyl	δ_{CH_2} Methylene	δ_{CH_2} Allyl	$\nu_{C=C}$ Ph	$\nu_{C=C}$ Allyl	$\nu_{C=O}$
Reactant	822	997	1032	1244	1291	1419	1458	1595	1648	
TS	815				1319		1434	1507	1542	
Keto-intermediate				1196	1300		1448	1555	1637	1720
Phenol product								1584	1635	

[a] Scaled using scaling factors shown in Table 1.

of the allyl group observed at 1650 cm^{-1} was red-shifted to 1580 cm^{-1} near a delay time of 750 fs.

The C–O bond was firstly weakened before generation of the six-membered structure. When the six-membered intermediate was generated, the C=C bond of the allyl group became an aromatic-like C=C bond observed at 1580 cm^{-1} (the C=C stretching mode of benzene is 1585 cm^{-1}). At a delay time of 1 ps, 6-allyl-cyclohexa-2,4-dienone was generated, as evidenced by a new peak due to carbonyl stretching at 1750 cm^{-1}. The peak at 1750 cm^{-1} disappeared at 2 ps, because the unstable 6-allyl-cyclohexa-2,4-dienone converted to the stable enol form. Thus, when the photon energy of the excitation light is lower than the minimum electronic transition energy, irradiation with few-optical-cycle pulses induces a photo-impulsive reaction in the EG state without converting photon energy to thermal energy, which is different from a traditional photoreaction.

4.3. Non-photo, non-thermal chemical reaction

In the case of the thermal Claisen rearrangement of APE, the activation energy was calculated to be about 33.9 kcal mol^{-1} using B3LYP/6-311 + G(d,p) (Fig. S1 in the ESI†). This value agrees with earlier reports.[13] Meanwhile, the few-optical-cycle visible pulses (λ = 525–725 nm) have the spectrum bandwidth of 5200 cm^{-1}. The bandwidth corresponds to ~14.5 kcal mol^{-1}, which is much lower than the activation energy of the thermal Claisen rearrangement. The reason why the Claisen rearrangement proceeds by the few-optical-cycle visible pulse is explained in the following.

The photo-impulsive reaction in the EG state excites some vibrational modes, which include modes related with the reaction. Therefore, the photo-impulsive reaction can proceed effectively with excitation energy lower than that of the thermal reaction exciting all of the vibrational modes. The photo-impulsive reaction in the EG state proceeds the reaction keeping coherence of the molecular vibrations, and it is no wonder that the activation barrier of the photo-impulsive reaction is different from that of the incoherent thermal reaction.

Meanwhile, the frontier orbitals of the photo-impulsive reaction in the EG state is thought to be same as those of the thermal reaction. Both of the two reactions have a same reaction pathway because the reaction mechanism is dominated by orbital symmetry.

The photo-impulsive reaction is thought to require the following two key factors to trigger the reaction.

(1) The width of the excitation pulse is much shorter than the molecular vibrational periods and should be as short as a few oscillation periods of the optical electric field (few-optical-cycle pulse).

(2) The photon energy of the excitation pulse should be lower than the minimum electronic transition energy.

Future challenges will focus on obtaining a definitive understanding of the driving mechanism for the reaction.

5. Conclusions

Traditional thermal reactions excite all vibrational modes of molecules in the reaction system. The photo-impulsive reaction induced with excitation of vibrational modes in the EG state with the few-optical-cycle pulse is coherently triggered. Induced Raman processes excite only a fraction of molecular vibrational modes to high level vibrational excited states. This results in only a fraction of molecules becoming "hot molecules" with highly excited vibrational states that trigger the reactions in the EG state. Hot molecules generally lose energy during collision with surrounding solvent molecules. In the present reaction, the chemical reaction of hot molecules proceeds within approximately 2 ps, which is much faster than collisions with surrounding molecules. The reaction presented in Fig. 4c follows the same reaction pathway as that of the symmetry-allowed thermal Claisen rearrangement in the EG state. Therefore, although the possibility of thermal reaction may not be completely ruled out, the photo-impulsively reaction in the EG

state with the few-optical-cycle pulse, which is neither a photoreaction nor a thermal reaction, is highly possible as a novel reaction scheme.

Acknowledgements

The authors thank the ITC of University of Electro-Communications for the computations in the theoretical calculations. This work was partly supported by Hayashi Memorial Foundation for Female Natural Science to I.I.

Notes and references

1 M. S. Kharasch, G. Stampa and W. Nudenberg, *Science*, 1952, **116**, 309; F. Galindo, *J. Photochem. Photobiol., C*, 2005, **6**, 123–138.
2 L. Claisen, *Ber. Dtsch. Chem. Ges.*, 1912, **45**, 3157–3166; A. M. M. Castro, *Chem. Rev.*, 2004, **104**, 2939–300.
3 I. Iwakura, A. Yabushita and T. Kobayashi, *Chem. Lett.*, 2010, **39**, 374–375.
4 I. Iwakura, A. Yabushita and T. Kobayashi, *Chem. Phys. Lett.*, 2011, **501**, 567–571.
5 The laser temperature-jump technique: E. Bemberg and P. Läuger, *J. Membr. Biol.*, 1973, **11**, 177–194; J. T. Knudtson and E. M. Eyring, *Annu. Rev. Phys. Chem.*, 1974, **25**, 255–274; W. Brock, G. Stark and P. S. Jordan, *Biophys. Chem.*, 1981, **13**, 329–348; G. Stark, M. Strässle and Z. Takácz, *J. Membr. Biol.*, 1986, **89**, 23–37; C. M. Phillips, Y. Mizutani and R. M. Hochstrasser, *Proc. Natl. Acad. Sci. U. S. A.*, 1995, **92**, 7292–7296; K. Yamamoto, Y. Mizutani and T. Kitagawa, *Biophys. J.*, 2000, **79**, 485–495; T. Yatsuhash and N. Nakashima, *Bull. Chem. Soc. Jpn.*, 2001, **74**, 579–593; J. Kubelka, *Photochem. Photobiol. Sci.*, 2009, **8**, 499–512.
6 The pressure-jump technique: M. Schiewek and A. Blume, *Eur. Biophys. J.*, 2009, **38**, 219–228; A. Blume and M. Hillmann, *Eur. Biophys. J.*, 1986, **13**, 343–353; K. Elamrani and A. Blume, *Biochemistry*, 1983, **22**, 3305–3311; J. Erbes, A. Gabke, G. Rapp and R. Winter, *Phys. Chem. Chem. Phys.*, 2000, **2**, 151–162.
7 The PH-jump technique: J. H. Clark, S. L. Shapiro, A. J. Campillo and K. R. Winn, *J. Am. Chem. Soc.*, 1979, **101**, 746–748; K. K. Smith, K. J. Kaufmann, D. Huppert and M. Gutman, *Chem. Phys. Lett.*, 1979, **64**, 522–527.
8 J. Liu, Y. Kida, T. Teramoto and T. Kobayashi, *Opt. Express*, 2010, **18**, 4664–4672.
9 A. Baltuska, T. Fuji and T. Kobayashi, *Opt. Lett.*, 2002, **27**, 306–308.
10 M. J. Frisch, G. W. Trucks, H. B. Schlegel, G. E. Scuseria, M. A. Robb, J. R. Cheeseman, J. A. Montgomery, Jr., T. Vreven, K. N. Kudin, J. C. Burant, J. M. Millam, S. S. Iyengar, J. Tomasi, V. Barone, B. Mennucci, M. Cossi, G. Scalmani, N. Rega, G. A. Petersson, H. Nakatsuji, M. Hada, M. Ehara, K. Toyota, R. Fukuda, J. Hasegawa, M. Ishida, T. Nakajima, Y. Honda, O. Kitao, H. Nakai, M. Klene, X. Li, J. E. Knox, H. P. Hratchian, J. B. Cross, V. Bakken, C. Adamo, J. Jaramillo, R. Gomperts, R. E. Stratmann, O. Yazyev, A. J. Austin, R. Cammi, C. Pomelli, J. W. Ochterski, P. Y. Ayala, K. Morokuma, G. A. Voth, P. Salvador, J. J. Dannenberg, V. G. Zakrzewski, S. Dapprich, A. D. Daniels, M. C. Strain, O. Farkas, D. K. Malick, A. D. Rabuck, K. Raghavachari, J. B. Foresman, J. V. Ortiz, Q. Cui, A. G. Baboul, S. Clifford, J. Cioslowski, B. B. Stefanov, G. Liu, A. Liashenko, P. Piskorz, I. Komaromi, R. L. Martin, D. J. Fox, T. Keith, M. A. Al-Laham, C. Y. Peng, A. Nanayakkara, M. Challacombe, P. M. W. Gill, B. Johnson, W. Chen, M. W. Wong, C. Gonzalez and J. A. Pople, *Gaussian 03, (Revision D.02)*, Gaussian, Inc., Wallingford CT.2004.
11 M. J. J. Vrakking, D. M. Villeneuve and A. Stolow, *Phys. Rev. A: At., Mol., Opt. Phys.*, 1996, **54**, R37–R40.
12 K. Heimi, *Chem. Pharm. Bull.*, 1974, **22**, 718.
13 S. Yamabe, S. Okumoto and T. Hayashi, *J. Org. Chem.*, 1996, **61**, 6218; B. Gmez, P. K. Chattaraj, E. Chamorro, R. Contreras and P. Fuentealba, *J. Phys. Chem. A*, 2002, **106**, 11227.